

1 **Modernizing the open-source community Noah-MP land surface model (version 5.0) with**
2 **enhanced modularity, interoperability, and applicability**

3
4 Cenlin He¹, Prasanth Valayamkunnath^{1,5}, Michael Barlage², Fei Chen¹, David Gochis¹, Ryan
5 Cabell¹, Tim Schneider¹, Roy Rasmussen¹, Guo-Yue Niu³, Zong-Liang Yang⁴, Dev Niyogi⁴,
6 Michael Ek¹

7
8 ¹National Center for Atmospheric Research (NCAR), Boulder, Colorado, USA
9 ²NOAA Environmental Modeling Center (EMC), College Park, Maryland, USA
10 ³University of Arizona, Tucson, Arizona, USA
11 ⁴University of Texas Austin, Austin, Texas, USA
12 ⁵Indian Institute of Science Education and Research Thiruvananthapuram, India

13
14
15 *Correspondence to:* Cenlin He (cenlinhe@ucar.edu)

16
17
18
19 **Abstract**

20
21 The widely-used open-source community Noah-MP land surface model (LSM) is designed for
22 applications ranging from uncoupled land-surface hydrometeorological and ecohydrological
23 process studies to coupled numerical weather prediction and decadal global/regional climate
24 simulations. It has been used in many coupled community weather/climate/hydrology models. In
25 this study, we modernize/refactor the Noah-MP LSM by adopting modern Fortran code standards
26 and data structures, which substantially enhances the model modularity, interoperability, and
27 applicability. The modernized Noah-MP is released as the version 5.0 (v5.0), which has five key
28 features: (1) enhanced modularization by re-organizing model physics into individual process-
29 level Fortran module files, (2) enhanced data structure with new hierarchical data types and
30 optimized variable declaration and initialization structures, (3) enhanced code structure and calling
31 workflow by leveraging the new data structure and modularization, (4) enhanced (descriptive and
32 self-explanatory) model variable naming standard, and (5) enhanced driver and interface structures
33 to couple with host weather/climate/hydrology models. In addition, we create a comprehensive
34 technical documentation of the Noah-MP v5.0 and a set of model benchmark and reference
35 datasets. The Noah-MP v5.0 will be coupled to various weather/climate/hydrology models in the
36 future. Overall, the modernized Noah-MP allows a more efficient and convenient process for
37 future model developments and applications.

Deleted: and standards

Deleted: and interoperability

Deleted: will

44 **1. Introduction**

45

46 Land surface models (LSMs) are useful modeling tools to resolve terrestrial responses to and
47 interactions with the atmosphere, ocean, glacier, and sea ice in the earth system. Traditionally,
48 LSMs were thought to mainly provide lower boundary conditions to the coupled atmospheric
49 models. However, modern LSMs have been increasingly employed as indispensable components
50 in the climate and weather systems to offer biogeophysical and biogeochemical insights for
51 understanding and quantifying the impact and evolution of climate, weather, and the integrated
52 earth environment (Blyth et al., 2021). LSMs have been widely applied to tackle many important
53 societally relevant challenges, such as drought, flood, heat wave, water availability, agriculture,
54 food security, wildfires, deforestation, and urbanization (Bonan and Doney, 2018).

55

56 Among many LSMs that have been developed in the past few decades, the open-source community
57 Noah with Multi-parameterization Options (Noah-MP; Niu et al., 2011; Yang et al., 2011) is one
58 of the most widely-used state-of-the-art LSMs. The article describing the Noah-MP model by Niu
59 et al (2011) is *de facto* the most cited LSM paper in the last 10 years, highlighting its worldwide
60 popular usage in the international science community. Compared to its predecessor, the Noah LSM
61 (Chen et al., 1996, 1997; Chen and Dudhia, 2001; Ek et al., 2003), Noah-MP significantly
62 improves known Noah limitations by employing enhanced treatments of vegetation canopy,
63 snowpack, soil processes, groundwater, and their complex interactions as well as additional
64 capabilities for critical land processes (e.g., crop, irrigation, tile drainage, groundwater, urban,
65 carbon and nitrogen cycles). Another unique feature of Noah-MP is the inclusion of multiple
66 physics options for different land processes, which allows the multi-physics model ensemble
67 experiments for uncertainty assessment and testing competing hypotheses (Zhang et al., 2016; J.
68 Li et al., 2020).

69

70 Noah-MP can be applied to various spatial scales spanning from point scale locally to ~100-km
71 resolution globally, and temporal scales spanning from sub-daily to decadal time scales. Since its
72 original development, Noah-MP has been used in many important applications, including
73 numerical weather prediction (Suzuki and Zupanski, 2018; Ju et al., 2022), high-resolution climate
74 modeling (Gao et al., 2017; Liu et al., 2017; Rasmussen et al., 2023), land data assimilation (Kumar
75 et al., 2019; Xu et al., 2021; Nie et al., 2022; Shu et al., 2022), drought (Arsenault et al., 2020; Niu
76 et al., 2020; Wu et al., 2021; Abolafia-Rosenzweig et al., 2023a), wildfire (Kumar et al., 2021;
77 Abolafia-Rosenzweig et al., 2022a, 2023b), snowpack evolution (Wrzesien et al., 2015; He et al.,
78 2019; Jiang et al., 2020), hydrology and water resources (Cai et al., 2014; Liang et al., 2019; X.
79 Zhang et al., 2022a; Hazra et al., 2023), crop and agricultural management (Liu et al., 2016;
80 Ingwersen et al., 2018; Warrach-Sagi et al., 2022; Valayamkunnath et al., 2022; Zhang et al., 2020,
81 2023), urbanization and heat island (Xu et al., 2018; Salamanca et al., 2018; Patel et al., 2022),
82 biogeochemical cycle (Cai et al., 2016; Brunsell et al., 2021), wind erosion (Jiang et al., 2021),

Deleted: an

84 wetland (Z. Zhang et al., 2022), groundwater (Barlage et al., 2015, 2021; Li et al., 2022), and
85 landslide hazard (Zhuo et al., 2019).

86

87 Currently, Noah-MP has been implemented into many community research and operational
88 weather/climate/hydrology models, including the Weather Research and Forecasting model
89 (WRF), the Model for Prediction Across Scales (MPAS), the NOAA operational National Water
90 Model (NWM), the NOAA Unified Forecast System (UFS), the NASA Land Information System
91 (LIS), and the NCAR High-Resolution Land Data Assimilation System (HRLDAS).

92

93 Despite its popular usage in the international research and application communities, the Noah-MP
94 core code engine was designed 12 years ago and is outdated, and does not take advantage of
95 modern Fortran language architecture. It has a single lengthy (>12,000 lines) Fortran source file
96 lumping together all model physics with complex code and data structures using inconsistent
97 format and does not follow the modern Fortran 2003 code standard ([https://j3-
98 fortran.org/doc/year/04/04-007.pdf](https://j3-
98 fortran.org/doc/year/04/04-007.pdf)). This makes the Noah-MP model code difficult for users and
99 developers to read, modify, and test as well as to implement and apply it to other community
100 models. Furthermore, a lengthy code is error prone and challenging to debug. These issues limit
101 the further development and application of Noah-MP.

102

103 Therefore, this effort is motivated to modernize (refactor) the entire Noah-MP model by adopting
104 modern Fortran 2003 code standards and data structures, which substantially enhances the model
105 modularity, interoperability, and applicability. The base code used for refactoring is the Noah-MP
106 version 4.5 (released in December 2022; [https://github.com/NCAR/noahmp/tree/release-v4.5-
107 WRF](https://github.com/NCAR/noahmp/tree/release-v4.5-
107 WRF)), and the refactoring effort does not change model physics. We release the
108 modernized/refactored Noah-MP as version 5.0 (v5.0; <https://github.com/NCAR/noahmp>), which
109 includes five key features: (1) enhanced modularization by re-organizing model physics into
110 individual process-level Fortran module files, (2) enhanced data structure with new hierarchical
111 data types and optimized variable declaration and initialization structures, (3) enhanced code
112 structure and subroutine calling workflow by leveraging the new data structure and modularization
113 and refining code to be more concise, (4) enhanced (descriptive and self-explanatory) model
114 variable naming standard, and (5) enhanced driver and interface code structures to couple with
115 host weather/climate/hydrology models. In addition, we have created a comprehensive technical
116 documentation (He et al., 2023) to describe model physics and details of the refactored Noah-MP
117 and a set of model benchmark and reference datasets for future comparison and assessment.
118 Overall, the modernized open-source community Noah-MP model (version 5.0) will allow a more
119 efficient and convenient process for future model developments and applications. The framework
120 and practice in the course of refactoring the entire Noah-MP code is also applicable to other LSMs
121 and ESMs.

122

Deleted: study

Deleted: and standards

Deleted: and interoperability

126 This paper reports the key features of the modernized Noah-MP v5.0 and is organized as follows.
127 Section 2 briefly summarizes the Noah-MP model physics with several updates since its original
128 development. Sections 3–7, respectively, introduce the key features of the modernized Noah-MP
129 in terms of enhanced model modularization, data type, code structure, variable naming, and
130 coupling structure with host models. Section 8 describes the model benchmarking and reference
131 datasets. Section 9 provides the release information of model code and technical documentation.
132 Section 10 concludes the paper with future model development plans.

134 2. Noah-MP version 5.0 model physics

136 2.1 Noah-MP description

137
138 Noah-MP (Niu et al., 2011) was originally developed based on the Noah LSM (Chen et al., 1996,
139 1997; Chen and Dudhia, 2001; Ek et al., 2003) to augment its modeling capabilities with enhanced
140 physical representations and treatments of dynamic vegetation, canopy interception and radiative
141 transfer processes, multi-layer snowpack physics, and soil and hydrological processes. The history
142 of model development and evolution has been described in the technical documentation (He et al.,
143 2023). Noah-MP is designed to simulate land surface and subsurface energy and water processes
144 in both uncoupled and coupled modes with atmospheric or hydrological models at sub-daily time
145 scale and high spatial resolution (even for point scale). This further allows the use of Noah-MP in
146 different hydrological, weather, and climate models for applications in a wide range of spatial and
147 temporal scales with proper integration in time and space.

148
149 The Noah-MP land grid is divided into two sub-grid tiles, namely vegetated and non-vegetated
150 grounds, based on vegetation cover fraction. The biogeophysical and biogeochemical processes
151 are treated separately for the vegetated and bare grounds. A “big-leaf” canopy treatment is adopted,
152 which is characterized by canopy properties dependent on vegetation types. Noah-MP accounts
153 for a multiple-layer snowpack, where snow ice and liquid water content, density, depth, and
154 temperature are simulated dynamically. There are also multi-layer soil thermal and hydrological
155 processes with dynamically evolving soil temperature and water content. The vegetation, snow,
156 and soil components in Noah-MP are closely coupled and interacted with each other via complex
157 energy, water, and biochemical processes. Their detailed physical formulations and
158 parameterizations in Noah-MP v5.0 are described in the technical documentation (He et al., 2023).
159 Below, we briefly summarize the energy, water, and biochemical processes in Noah-MP v5.0.

161 2.2 Noah-MP energy processes

162
163 Noah-MP resolves energy budgets and processes separately for vegetated and non-vegetated
164 ground portions of each grid (Niu et al., 2011). The vegetation cover fraction, either from
165 observational inputs or model calculations based on leaf area index (LAI) inputs or predicted by

Deleted: divides its

Deleted: Noah-MP adopts a

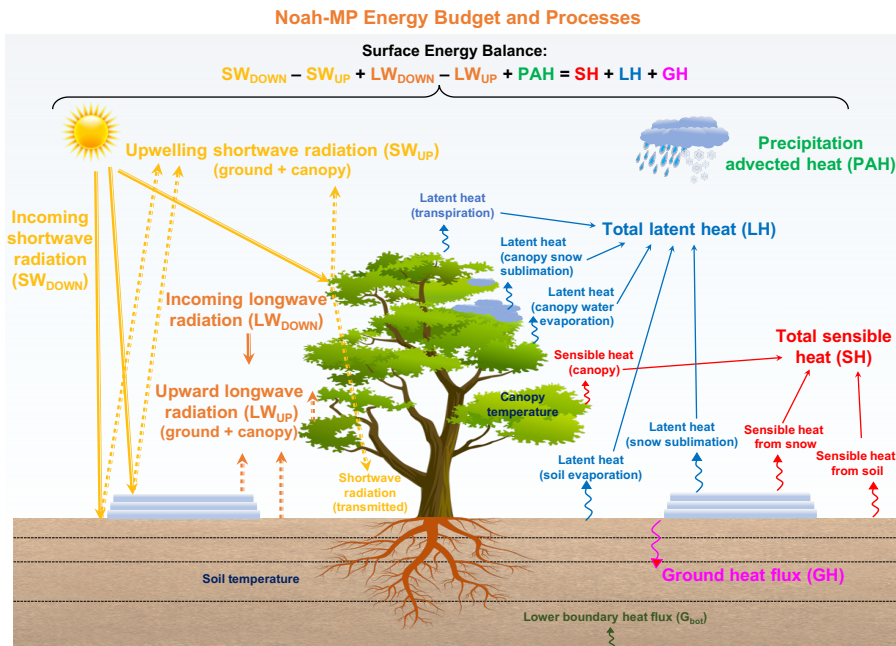
Deleted: Noah-MP also includes

169 the dynamic vegetation module, is used to separate vegetated and bare grounds. The grid-mean
170 energy states and fluxes are calculated as an average of vegetated and bare ground values weighted
171 by vegetation cover fraction. For surface radiative processes driven by incoming shortwave and
172 longwave radiation (atmospheric forcing), Noah-MP simulates the radiative absorption and
173 scattering by the canopy and ground (soil/snow) as well as the longwave emissions by the canopy
174 and ground (soil/snow). The net absorbed total (shortwave and longwave) radiative flux is
175 balanced by precipitation advected heat flux, total surface sensible and latent heat fluxes, and
176 ground heat flux. The precipitation advected heat flux represents the heat flux advected from
177 precipitation (rain/snow) to canopy/ground due to the temperature difference between precipitation
178 (surface air) and canopy/ground. The total surface sensible heat includes the sensible heat from
179 canopy, snowpack, and soil surfaces. The total surface latent heat includes the latent heat from
180 snowpack sublimation, soil evaporation, canopy snow sublimation, canopy water evaporation, and
181 plant transpiration. The ground heat flux is the heat flux leaving the ground surface to drive
182 subsurface snow/soil phase change and/or temperature changes.

183

184 To model the aforementioned surface energy flux components, Noah-MP dynamically calculates
185 a number of key land surface properties, include ground snow cover fraction, surface roughness,
186 canopy and ground thermal properties, snow and soil albedo, surface emissivity, and canopy
187 radiative transfer. Many of these property and process calculations have multiple physics options
188 (see Sect. 2.6). Based on the canopy and ground energy balance, Noah-MP further solves the
189 temperature and phase change for canopy, snowpack, and soil. Figure 1 summarizes the key energy
190 processes and budget components as well as the energy balance equation in Noah-MP v5.0. Note
191 that the energy processes at glacier grids are treated similarly to those at 100% bare (non-vegetated)
192 ground grids except that the soil is replaced by glacier ice with ice-specific properties.

193



194
 195 **Figure 1.** Schematic diagram of energy budget and processes represented in Noah-MP version 5.0.
 196

197

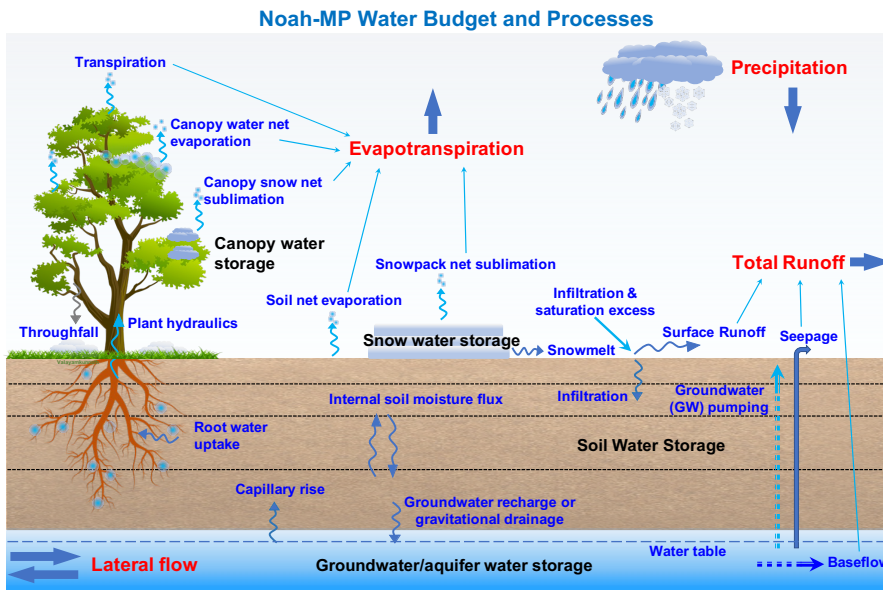
198

2.3 Noah-MP water processes

199

200 Noah-MP accounts for five major water budget components, including precipitation,
 201 evapotranspiration (ET), total runoff, net lateral flow, and total water storage change intercepted
 202 by the canopy and in snow, soil, and aquifer. For precipitation, Noah-MP has several temperature-
 203 based rainfall-snowfall partitioning parameterizations or can use the partitioning from atmospheric
 204 models directly (see Sect. 2.6). Noah-MP simulates canopy interception and throughfall of rain
 205 and snow, where the intercepted rain and snow on the canopy can go through unloading/dripping,
 206 frost, sublimation, melting, and freezing processes. Net evaporation loss from the canopy-
 207 intercepted liquid water (evaporation minus dew), net sublimation from the canopy-intercepted
 208 snow (sublimation minus frost), transpiration (via plant hydraulics), net soil surface evaporation,
 209 and net snowpack sublimation together contribute to the total surface ET. Noah-MP dynamically
 210 simulates multi-layer snowpack water storage (ice and liquid water) changes driven by
 211 snowfall/rainfall, frost, sublimation, freezing, and melting. The snowmelt water out of snowpack
 212 together with rainfall at the soil surface are further partitioned into surface runoff and infiltration
 213 based on multiple runoff and infiltration physics options (see Sect. 2.6). Soil moisture and

214 unsaturated water flow across soil layers are simulated using the one-dimensional Richards
 215 equation. Two optional groundwater schemes, one without 2-D lateral flow (Niu et al., 2007) and
 216 one with 2-D lateral flow (Fan et al., 2007; Miguez-Macho et al. 2007), are available in Noah-MP
 217 to simulate groundwater dynamics, including groundwater recharge, water table change, baseflow,
 218 seepage, and/or lateral flow. Noah-MP also includes dynamic irrigation and tile drainage processes
 219 for agricultural management applications (Valayamkunnath et al., 2021, 2022). Figure 2
 220 summarizes the key water processes and budget components as well as the water balance equation
 221 in Noah-MP v5.0. Note that the water processes at glacier grids are treated similarly to those at
 222 100% bare ground grids except that all the soil and subsurface hydrological processes are removed
 223 and replaced by glacier ice (He et al., 2023).
 224



Total water balance:

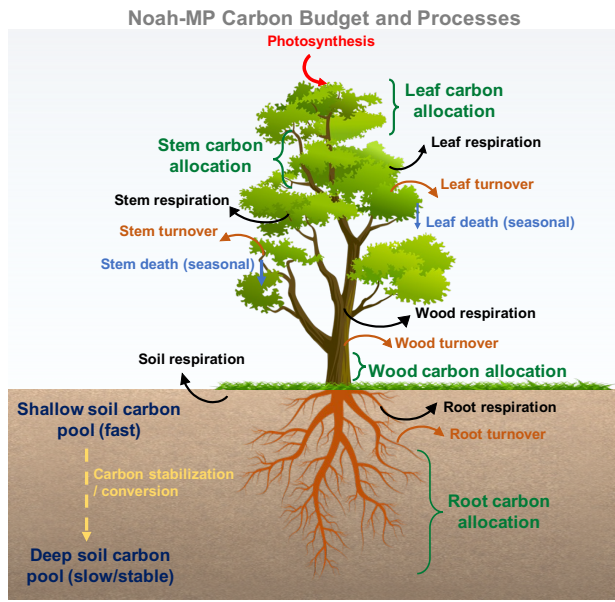
$$\text{Precipitation} + \text{lateral flow} - \text{Evapotranspiration} - \text{Total Runoff} = \Delta (\text{water storage in canopy, snow, soil, aquifer})$$

225
 226 **Figure 2.** Schematic diagram of water budget and processes represented in Noah-MP version 5.0.
 227

228
 229 **2.4 Noah-MP biochemical processes**
 230

231 Currently, the community version of Noah-MP only accounts for carbon processes for biochemical
 232 cycles, while nitrogen dynamics and soil carbon dynamics have been developed in non-community
 233 Noah-MP versions managed by individual research groups (e.g., Cai et al., 2016; X. Zhang et al.,

234 2022b). We will synthesize and integrate individual Noah-MP updates into the community version
 235 in the future (see Sect. 2.5 for more discussions). Noah-MP simulates carbon processes for both
 236 natural/generic vegetation (Niu et al., 2011) and explicit agricultural crops (Liu et al., 2016). The
 237 carbon processes related to vegetation growth dynamics include (1) carbon assimilation from
 238 photosynthesis by shaded and sunlit leaves, (2) carbon allocation to different parts of vegetation
 239 (leaf, stem, wood and root) and soil carbon pools (fast and slow carbon), (3) carbon loss due to
 240 respiration of different vegetation and soil carbon pools, (4) carbon transfer between vegetation
 241 and fast soil carbon pools through vegetation (leaf, stem, wood and root) turnover and seasonal
 242 death of leaf and stem, and (5) soil carbon pool conversion through soil carbon stabilization. The
 243 total carbon flux to the atmosphere and net primary productivity are computed based on the
 244 aforementioned carbon processes. Figure 3 summarizes the key carbon processes and budget
 245 components as well as the carbon balance equation in Noah-MP v5.0. Note that the carbon
 246 processes for crop growth are treated similarly to those of natural vegetation, except that the wood
 247 component of plants is removed and the grain component of crops is added with additional carbon
 248 conversion from leaf, stem, and root to grain depending on crop growing stages.
 249



Total carbon balance:

$$\text{Photosynthesis} - \text{Respiration} = \Delta \text{Plant carbon pool} + \Delta \text{Soil carbon pool}$$

250
 251 **Figure 3.** Schematic diagram of carbon budget and processes represented in Noah-MP version 5.0.
 252

253

254 **2.5 Noah-MP physics updates since original development**

255

256 Since the release of the original Noah-MP in year 2011 (Niu et al., 2011), there are several
257 important updates in Noah-MP physics. Some of the updates have been included in the community
258 version of Noah-MP v5.0, while some are only available in the non-community versions managed
259 by individual research groups. We will make efforts to synthesize and integrate individual Noah-
260 MP updates into the community version in the future by working with those developer teams. Here,
261 to the best of our knowledge, we briefly list the major Noah-MP physics updates from the
262 community in the past decade.

263

264 The new/enhanced physics included in the community Noah-MP version 5.0 since 2011 are: (1)
265 the Miguez-Macho-Fan (MMF) groundwater scheme (Barlage et al., 2015); (2) three additional
266 runoff schemes: the Variable infiltration capacity (VIC), dynamic VIC, and Xinanjiang schemes
267 (McDaniel et al., 2020); (3) tile drainage schemes (Valayamkunnath et al., 2022); (4) dynamic
268 irrigation schemes (sprinkler, micro, and flooding irrigation) (Valayamkunnath et al., 2021); (5) a
269 dynamic crop growth model for corn and soybean (Liu et al., 2016) with enhanced C3 and C4 crop
270 parameters (Zhang et al., 2020); (6) coupling with urban canopy models (Xu et al., 2018;
271 Salamanca et al., 2018) with local climate zone modeling capabilities (Zonato et al., 2021); (7)
272 enhanced snow cover, snow compaction, and wind-canopy absorption parameters (He et al., 2021);
273 (8) a wet-bulb temperature-based snow-rain partitioning scheme (Wang et al., 2019).

274

275 The new/enhanced physics currently not included in the community Noah-MP version 5.0 since
276 2011 are: (1) nitrogen dynamics (Cai et al., 2016); (2) big-tree plant hydraulics (Li et al., 2021);
277 (3) dynamic root optimization (Wang et al. 2018) with an explicit representation of plant water
278 storage (Niu et al., 2020); (4) additional snow cover parameterizations (Jiang et al., 2020); (5)
279 coupling with a wind erosion model (Jiang et al., 2021); (6) a wetland representation and dynamics
280 (Z. Zhang et al., 2022); (7) a unified turbulence parameterization throughout the canopy and
281 roughness sublayer (Abolafia-Rosenzweig et al., 2021); (8) enhanced snow albedo representations
282 (Abolafia-Rosenzweig et al., 2022b); (9) coupling with a snow radiative transfer (SNICAR) model
283 (Wang et al., 2020, 2022); (10) an organic soil layer representation at forest floors (Chen et al.,
284 2016) and a microbial-explicit soil organic carbon decomposition model (MESDM; X. Zhang et
285 al., 2022b); (11) coupling with atmospheric dry deposition of air pollutant (Chang et al., 2022);
286 (12) enhanced permafrost soil representations (X. Li et al., 2020); (13) spring wheat crop dynamics
287 (Zhang et al., 2023); (14) new treatment of thermal roughness length (Chen and Zhang 2009); (15)
288 the Gecros crop model (Ingwersen et al., 2018; Warrach-Sagi et al., 2022); (16) a 1-D dual-
289 permeability flow model (based on the mixed-form Richards' equation) representing preferential
290 flow through variably-saturated soil with surface ponding being developed ~~at~~ the University of
291 Arizona.

292

293 **2.6 Noah-MP multi-physics options**

Deleted: in

295

296 One unique feature and advantage of Noah-MP is the inclusion of multiple physics options for
 297 different land processes for testing competing hypotheses (i.e., options) and multi-model ensemble
 298 simulations. Table 1 summarizes all the available physics options in the community Noah-MP
 299 v5.0. In particular, compared to previous Noah-MP versions, we have separated the runoff options
 300 for surface and subsurface runoff processes, and added a new physics option for snow thermal
 301 conductivity calculations, which were originally hard-coded without the namelist control
 302 capability. More detailed descriptions of each physics option are provided in the technical
 303 documentation (He et al., 2023).

304

305

Table 1. List of Noah-MP version 5.0 multi-physics options

Noah-MP Physics	Option	Notes (* indicates the default option)
OptDynamicVeg options for dynamic (prognostic) vegetation	1	off (use table LeafAreaIndex; use VegFrac = VegFracGreen from input) (Niu et al., 2011; Yang et al., 2011)
	2	on (together with OptStomataResistance = 1) (Dickinson et al., 1998; Niu and Yang, 2003)
	3	off (use table LeafAreaIndex; calculate VegFrac)
	4*	off (use table LeafAreaIndex; use maximum vegetation fraction)
	5	on (use maximum vegetation fraction)
	6	on (use VegFrac = VegFracGreen from input)
	7	off (use input LeafAreaIndex; use VegFrac = VegFracGreen from input)
	8	off (use input LeafAreaIndex; calculate VegFrac)
	9	off (use input LeafAreaIndex; use maximum vegetation fraction)
OptRainSnowPartition options for partitioning precipitation into rainfall & snowfall	1*	Jordan (1991) scheme
	2	BATS: when TemperatureAirRefHeight < freezing point+2.2 (Yang and Dickinson, 1996)
	3	TemperatureAirRefHeight < freezing point (Niu et al., 2011)
	4	Use WRF microphysics output (Barlage et al., 2015)
	5	Use wet-bulb temperature (Wang et al., 2019)
OptSoilWaterTranspiration options for soil moisture factor for stomatal resistance & ET	1*	Noah (soil moisture) (Ek et al., 2003)
	2	CLM (matric potential) (Oleson et al., 2004)
	3	SSiB (matric potential) (Xue et al., 1991)
OptGroundResistanceEvap options for ground resistant to evaporation/sublimation	1*	Sakaguchi and Zeng (2009) scheme
	2	Sellers (1992) scheme
	3	adjusted Sellers (1992) for wet soil
	4	Sakaguchi and Zeng (2009) for non-snow; rsurf = rsurf_snow for snow (set in NoahmpTable.TBL)
OptSurfaceDrag options for surface layer drag/exchange coefficient	1*	Monin-Obukhov (M-O) Similarity Theory (Brutsaert, 1982)
	2	original Noah (Chen et al. 1997)

OptStomataResistance	1*	Ball-Berry scheme (Ball et al., 1987; Bonan, 1996)
options for canopy stomatal resistance	2	Jarvis scheme (Jarvis, 1976)
OptSnowAlbedo	1*	BATS snow albedo (Dickinson et al., 1993)
options for ground snow surface albedo	2	CLASS snow albedo (Verseghy, 1991)
OptCanopyRadiationTransfer	1	modified two-stream ($gap = f(\text{solar angle, 3D structure, etc}) < 1 - \text{VegFrac}$) (Niu and Yang, 2004)
options for canopy radiation transfer	2	two-stream applied to grid-cell ($gap=0$) (Niu et al., 2011)
	3*	two-stream applied to vegetated fraction ($gap=1 - \text{VegFrac}$) (Dickinson, 1983; Sellers, 1985)
OptSnowSoilTempTime	1*	semi-implicit; flux top boundary condition (Niu et al., 2011)
options for snow/soil temperature time scheme (only layer 1)	2	full implicit (original Noah); temperature top boundary condition (Ek et al., 2003)
	3	same as 1, but snow cover for skin temperature calculation (Niu et al., 2011)
OptSnowThermConduct	1*	Stieglitz scheme (Yen, 1965)
options for snow thermal conductivity	2	Anderson (1976) scheme
	3	Constant (Niu et al., 2011)
	4	Verseghy (1991) scheme
	5	Douville scheme (Yen, 1981)
OptSoilTemperatureBottom	1	zero heat flux from bottom (DepthSoilTempBottom & TemperatureSoilBottom not used) (Niu et al., 2011)
options for lower boundary condition of soil temperature	2*	TemperatureSoilBottom at DepthSoilTempBottom (8m) read from a file (original Noah) (Ek et al., 2003)
OptSoilSupercoolWater	1*	No iteration (Niu and Yang, 2006)
options for soil supercooled liquid water	2	Koren's iteration (Koren et al., 1999)
OptRunoffSurface	1	TOPMODEL with groundwater (Niu et al., 2007)
	2	TOPMODEL with an equilibrium water table (Niu et al., 2005)
	3*	Schaake scheme (original Noah) (Schaake et al., 1996)
	4	BATS surface and subsurface runoff (Yang and Dickinson, 1996)
	5	Miguez-Macho & Fan (MMF) groundwater scheme (Fan et al., 2007; Miguez-Macho et al. 2007)
	6	Variable Infiltration Capacity Model surface runoff scheme (Liang et al., 1994)
	7	Xinjiang Infiltration and surface runoff scheme (Jayawardena and Zhou, 2000)
	8	Dynamic VIC surface runoff scheme (Liang and Xie, 2003)

OptRunoffSubsurface options for drainage & subsurface runoff	1~8	similar to runoff option, separated from original Noah-MP runoff option, currently tested & recommended the same option# as surface runoff (default)
OptSoilPermeabilityFrozen options for frozen soil permeability	1*	linear effects, more permeable (Niu and Yang, 2006)
	2	nonlinear effects, less permeable (Koren et al., 1999)
OptDynVicInfiltration options for infiltration in dynamic VIC runoff scheme	1*	Philip scheme (Liang and Xie, 2003)
	2	Green-Ampt scheme (Liang and Xie, 2003)
	3	Smith-Parlange scheme (Liang and Xie, 2003)
OptTileDrainage options for tile drainage currently only tested & calibrated to work with runoff option=3	0*	No tile drainage
	1	on (simple scheme) (Valayamkunnath et al., 2022)
	2	on (Hooghoudt's scheme) (Valayamkunnath et al., 2022)
OptIrrigation options for irrigation	0*	No irrigation
	1	Irrigation on (Valayamkunnath et al., 2021)
	2	irrigation trigger based on crop season planting and harvesting dates (Valayamkunnath et al., 2021)
	3	irrigation trigger based on LeafAreaIndex threshold (Valayamkunnath et al., 2021)
OptIrrigationMethod options for irrigation method, only works when OptIrrigation > 0	0*	method based on geo_em fractions
	1	sprinkler method (Valayamkunnath et al., 2021)
	2	micro/drip irrigation (Valayamkunnath et al., 2021)
	3	surface flooding (Valayamkunnath et al., 2021)
OptCropModel options for crop model	0*	No crop model
	1	Liu, et al. (2016) crop scheme
OptSoilProperty options for defining soil properties	1*	use input dominant soil texture
	2	use input soil texture that varies with depth
	3	use soil composition (sand, clay, orgm) and pedotransfer function
	4	use input soil properties
OptPedotransfer options for pedotransfer functions, only works when OptSoilProperty=3	1*	Saxton and Rawls (2006) scheme
OptGlacierTreatment options for glacier treatment	1*	include phase change of glacier ice
	2	Glacier ice treatment more like original Noah

306

307

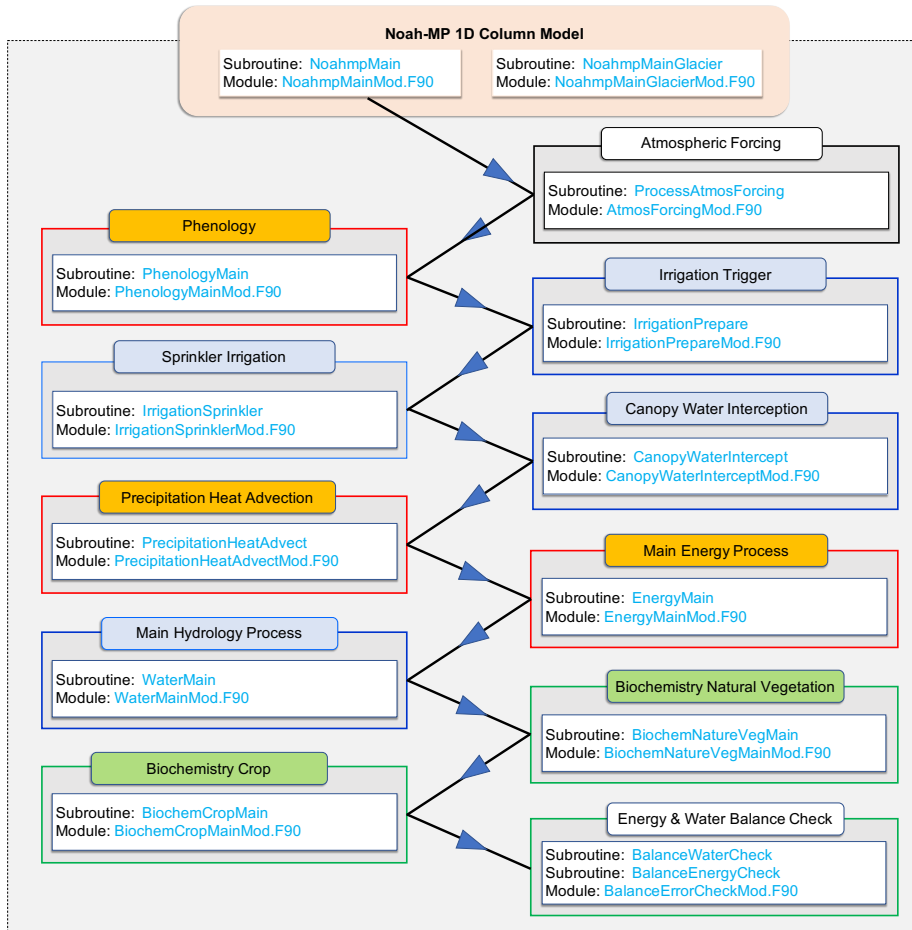
308 3. Enhanced model modularization in Noah-MP version 5.0

309

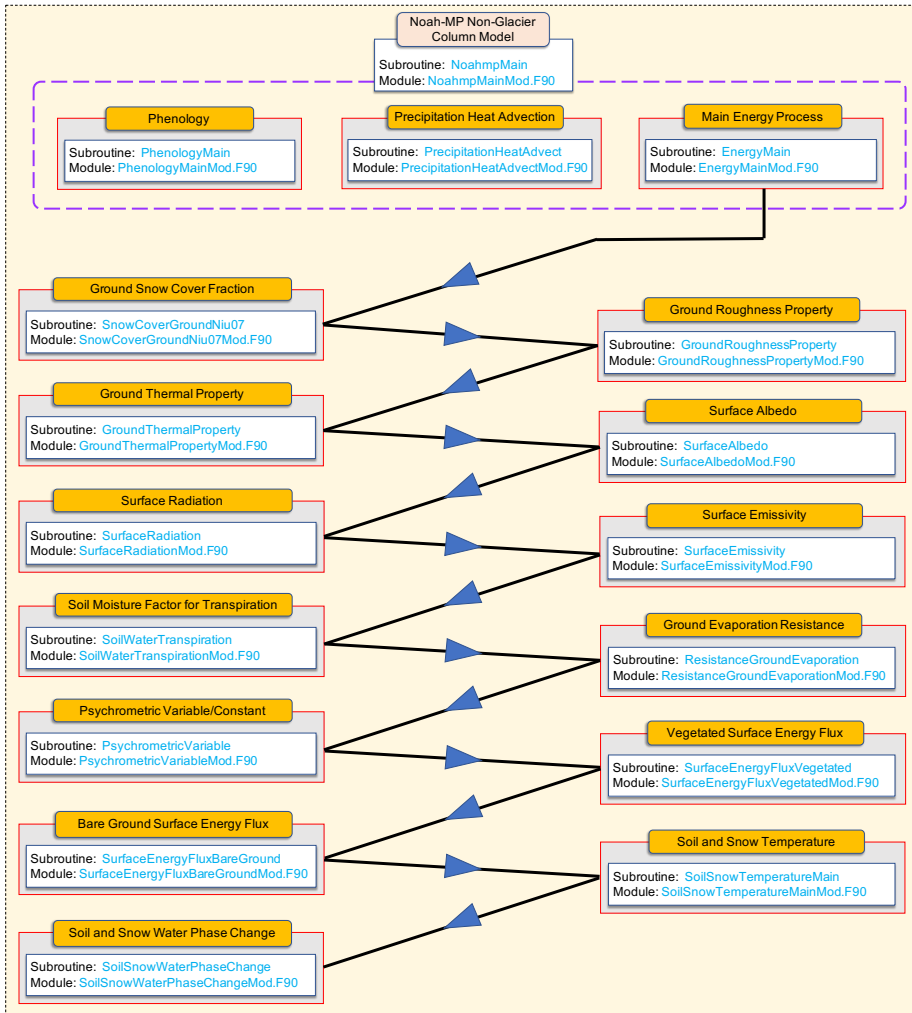
310 In the Noah-MP v5.0, we have modularized all model physics by separating and re-organizing
311 each code subroutine into individual process-level Fortran module file with new descriptive, self-

312 explanatory module and subroutine names. As such, each model physics or scheme has its own
313 separate module. Figure 4 shows the calling tree of the modularized Noah-MP main model physics
314 workflow. Figures 5-7 show the calling tree of the modularized energy, water, and carbon
315 processes, respectively. Compared to the previous Noah-MP versions that have a single lengthy
316 source file lumping together all model subroutines with non-self-explanatory names, the highly-
317 modularized model structure of the Noah-MP v5.0 provides a much more clear, neat, and
318 organized way for users and developers to understand and follow the model logics and physics.
319 These new modules use consistent coding format and standards, offering convenience for code
320 reading, writing, and debugging. The highly-modularized model structure facilitates future
321 development by allowing specific model physics to be worked in isolation or replaced without
322 interfering with other parts of the model code. This modularization also allows external community
323 weather/climate/hydrology models to easily adopt specific Noah-MP physical processes/schemes
324 as independent process-level module files and implement them for testing and coupling.

325

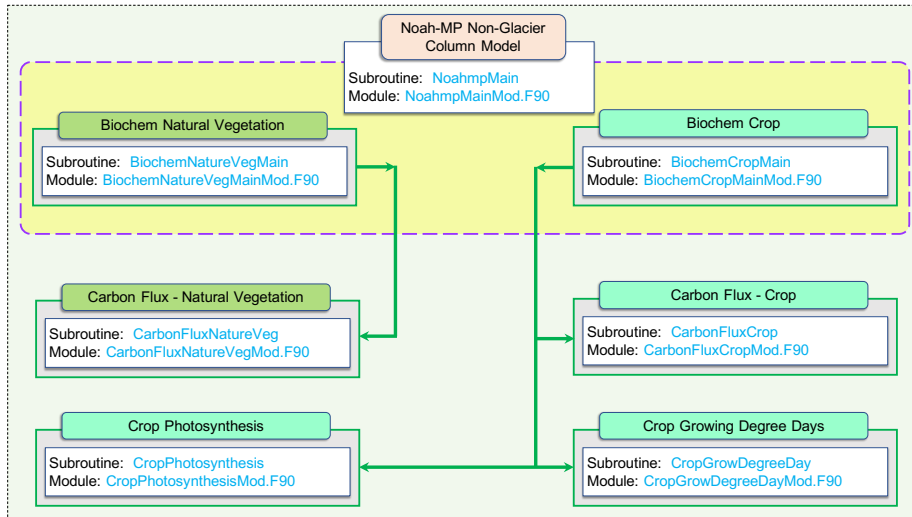


326
 327 **Figure 4.** The modularized Noah-MP main physics calling tree in version 5.0. Blue boxes indicate
 328 water processes, orange boxes indicate energy processes, and green boxes indicate biochemical
 329 processes. The direction of arrows indicates processes calling sequence and information flow. Note
 330 that the 1-D glacier column model has similar structures as the main non-glacier model, except
 331 that the vegetation-related processes are removed and soil is replaced by glacier ice.
 332



333
 334
 335
 336
 337

Figure 5. The modularized Noah-MP energy processes calling tree in version 5.0. Note that the glacier model has similar structures except that the vegetation-related processes are removed and soil is replaced by glacier ice.



343

344

345

346

347

348

349

350

351

Figure 7. The modularized Noah-MP biochemical processes calling tree in version 5.0. Note that currently the Noah-MP v5.0 only includes carbon processes. Note that the CropPhotosynthesis module is not used currently to avoid inconsistency with the photosynthesis calculations from the canopy stomatal resistance module.

4. Enhanced data structure in Noah-MP version 5.0

352

353

354

355

356

357

358

359

360

361

362

363

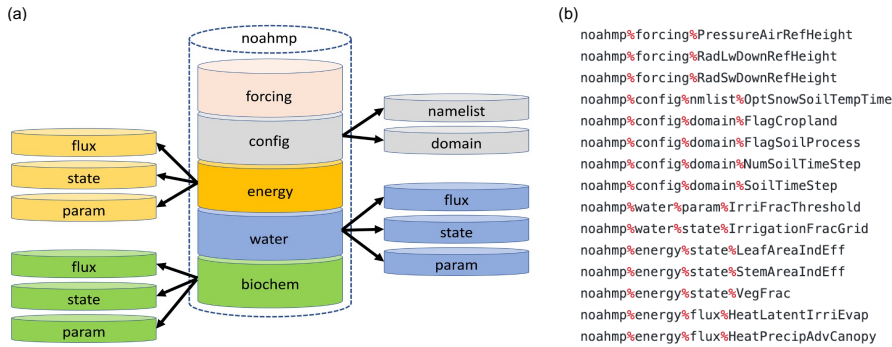
364

365

In the Noah-MP v5.0, we have enhanced data structure with new hierarchical data types, which allows a more efficient and convenient control of model variables and substantially simplifies code structures and calling interface (Section 5). Figure 8 summarizes the new Noah-MP data type hierarchy and gives some examples of model variable expression based on the hierarchical data types. Specifically, we have defined an overarching “noahmp” main data type, which includes “forcing” for atmospheric forcing variable type, “config” for model configuration variable type with “domain” and “namelist” subtypes, “energy” for energy-related variable type, “water” for water-related variable type, and “biochem” for biochemistry-related variable type. The “energy”, “water”, and “biochem” types are further divided into “flux”, “state”, and “param” subtypes for flux, state, and parameter variables. This hierarchical data structure provides a better organization and management of model variables and their physical attributes. We have also optimized the variable declaration and initialization structures based on those new data types and consistent coding format and standard. In addition, we have re-defined many key local model state, flux, and parameter variables in the base code to be global variables in the refactored code, which allows a

366 better track and management of these variables for diagnosis, transfer between Noah-MP and host
 367 models, and coupling with data assimilation systems.

368
 369



370
 371 **Figure 8.** (a) The new hierarchical “noahmp” data types in the Noah-MP version 5.0. (b) Examples
 372 of model variable expression using the hierarchical data types.

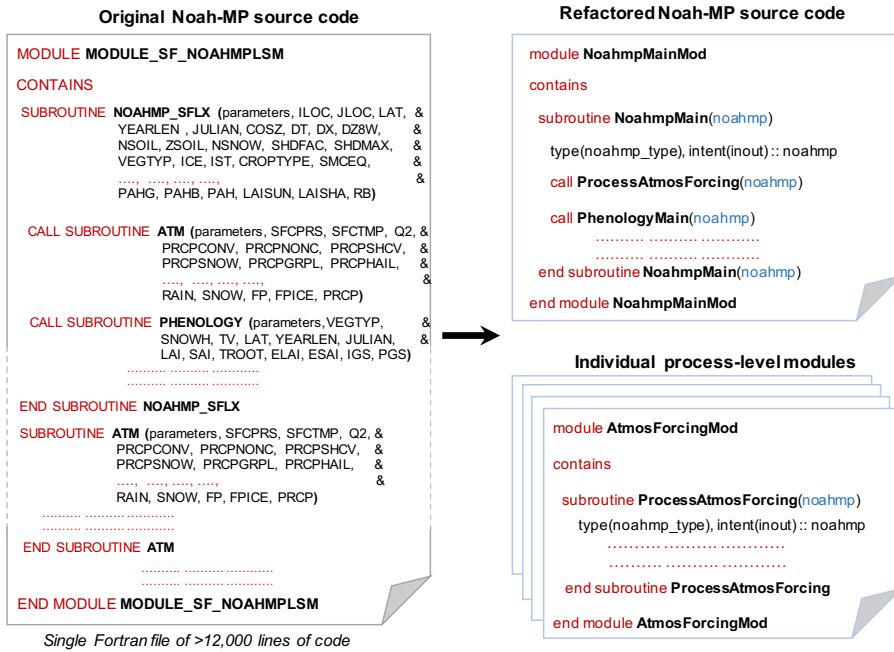
373
 374

375 5. Enhanced code structure in Noah-MP version 5.0

376

377 Leveraging the model modularization (Section 3) and new data types (Section 4) in the Noah-MP
 378 v5.0, we have further refined the code structure and subroutine interface. A graphical
 379 representation of the refactored Noah-MP subroutine interface is depicted in Figure 9. Specifically,
 380 the refined subroutine interface only requires passing the “noahmp” data type instead of each
 381 individual variable names, because all relevant variables are defined and included in the “noahmp”
 382 data type. This significantly simplifies the code structure with much more concise and neat
 383 subroutine calls. The refined subroutine interface also makes future model development and code
 384 changes simpler, more efficient, and less error-prone. For instance, if users want to add/remove a
 385 variable for a specific physical scheme, they only need to edit as few as 3 module files: variable
 386 type definition module, variable initialization module, the target physical scheme module, and if
 387 needed, the variable input/output module. There is no need to go through and change all the
 388 subroutine calls and interfaces that use the target variable.

389



390
391 **Figure 9.** Demonstration of refactored subroutine interface and code structure in the Noah-MP
392 version 5.0.

393
394
395 **6. Enhanced variable naming in Noah-MP version 5.0**

396
397 In the Noah-MP v5.0, we have also renamed all the model variables using a more descriptive and
398 self-explanatory naming standard, which clarifies the physical meaning of variables directly by
399 their names and hence substantially lowers the hurdles of reading and understanding the code and
400 model physics. The original variable names in the previous Noah-MP versions are hard to
401 understand, in which case users have to check back and forth the variable definition to know their
402 physical meaning. For instance, the original variable name for canopy intercepted total water is
403 “CMC”, while the new name is “CanopyTotalWater”. Table 2 gives more examples of the
404 enhanced variable naming in Noah-MP v5.0. A detailed Noah-MP variable glossary listing
405 variables’ original and new names, physical meaning, data type, and unit is provided in the
406 technical documentation (He et al., 2023) and the community Noah-MP GitHub repository.

410 **Table 2.** Examples of new variable names based on a more descriptive and self-explanatory
 411 naming standard in the Noah-MP version 5.0, compared with the original names.

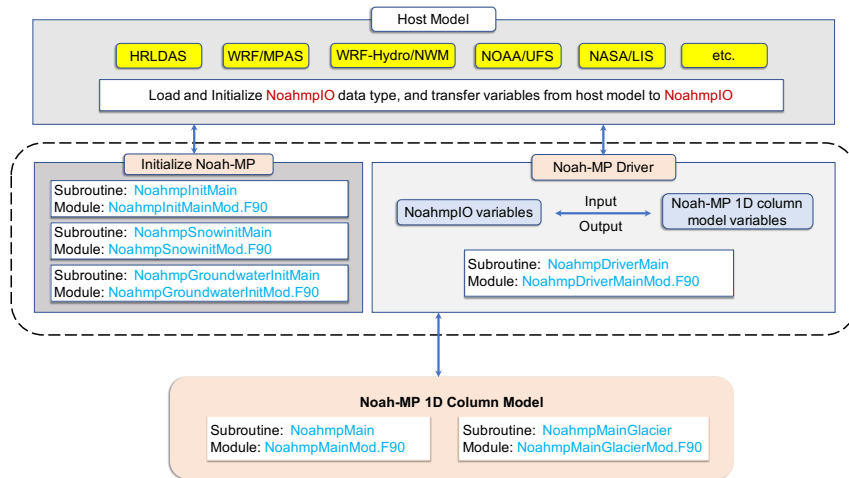
Variable physical meaning/definition	New name	Original name	Variable Type	Unit
wetted or snowed fraction of canopy	CanopyWetFrac	FWET	Real	-
canopy intercepted liquid water	CanopyLiqWater	CANLIQ	Real	mm
canopy intercepted ice	CanopyIce	CANICE	Real	mm
canopy intercepted total water	CanopyTotalWater	CMC	Real	mm
canopy capacity for snow interception	CanopyIceMax	MAXSNO	Real	mm
canopy capacity for liquid water interception	CanopyLiqWaterMax	MAXLIQ	Real	mm
ice fraction in snow layers	SnowIceFrac	FICE_SNOW	Real	-
bulk density of snowfall	SnowfallDensity	BDFALL	Real	kg/m ³
snow cover fraction	SnowCoverFrac	FSNO	Real	-
snow layer ice	SnowIce	SNICE	Real	mm
snow layer liquid water	SnowLiqWater	SNLIQ	Real	mm

412
 413
 414
 415

7. Enhanced coupling structure with host models in Noah-MP version 5.0

416 We have further updated the Noah-MP driver and interface coupled with potential host
 417 weather/climate/hydrology models. Figure 10 summarizes the interface and coupling structures in
 418 the Noah-MP v5.0. Specifically, the coupling interface includes: (1) defining a 2-D (for structured
 419 grid mesh) or vectorized (for unstructured grid mesh) Noah-MP input/output data type
 420 “NoahmpIO” to facilitate the input/output communication between host models and the core
 421 Noah-MP 1-D column model (“noahmp” data type); (2) the initialization of the “NoahmpIO”
 422 variables with values from host models; (3) the main Noah-MP driver that calls the core 1-D
 423 column model and transfers between the “NoahmpIO” and “noahmp” variables as part of
 424 input/output processes. Currently, the coupling of the Noah-MP v5.0 with the NCAR/HRLDAS
 425 system has been successfully completed. The coupling of Noah-MP v5.0 with the NASA/LIS
 426 system and the WRF-Hydro/NWM system is on-going. We also plan to couple the Noah-MP v5.0
 427 with other host models in the future (Section 9), such as WRF, MPAS, and NOAA/UFS. Because
 428 of the enhanced coupling interface and structure in Noah-MP v5.0, we will only need to slightly
 429 adapt the coupling interface and driver to allow it to work with different host models. We will
 430 manage and maintain the interface and driver code for each host model in the community Noah-
 431 MP GitHub repository to ensure the compatibility between host models and updated core Noah-
 432 MP source code in the future, which will allow smooth transition and seamless synthesizing of
 433 Noah-MP updates in host models.

434



435
 436 **Figure 10.** Workflow of the Noah-MP v5.0 driver and interface structures to couple with various
 437 host weather/climate/hydrology models.
 438

439
 440

8. Benchmarking for Noah-MP version 5.0

441

442 To benchmark the functionality, reproducibility, and computational efficiency of the modernized
 443 Noah-MP code, we have conducted a series of hierarchical test simulations during the course of
 444 Noah-MP refactoring. Specifically, after refactoring each major Noah-MP model
 445 component/physics (e.g., water, energy, carbon, etc.) listed in Figure 4, we built simple driver
 446 modules to conduct benchmark simulations using each of these model component/physics to test
 447 and ensure the bit-for-bit consistency between the refactored code and base code for all Noah-MP
 448 physics options. Here is an example for the refactored Noah-MP water component model we built
 449 for benchmarking during the course of refactoring:
 450 https://github.com/cenlinhe/NoahMP_refactor/tree/water_refactor, which was used to test the bit-
 451 for-bit consistency between the refactored and base Noah-MP water component codes.

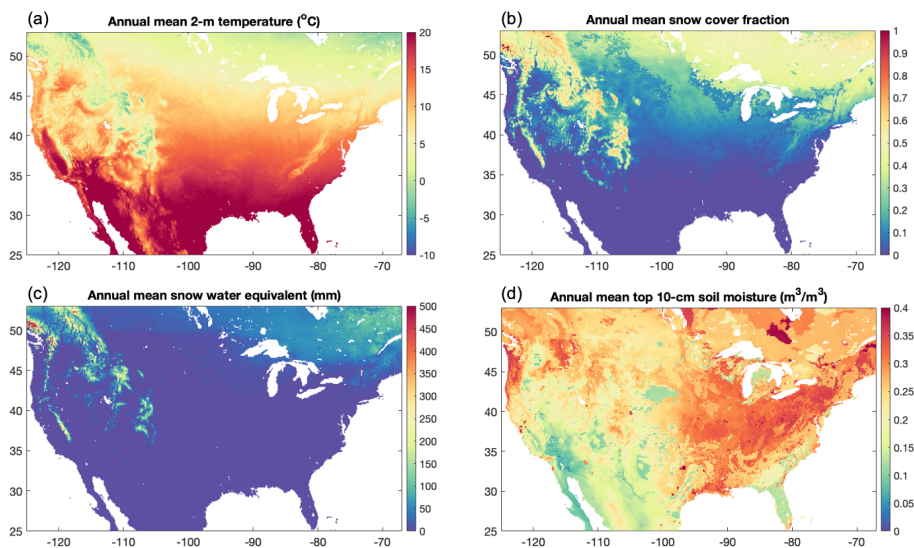
452

453 After we completed the entire model refactoring, we have conducted another set of test simulations
 454 using the completed Noah-MP v5.0 to ensure its bit-for-bit consistency with the base model code
 455 for all different combinations of physics options as well as to benchmark its computational
 456 efficiency. These tests were conducted via 1-year point-scale SNOTEL 804-site simulations, 1-
 457 year 12-km gridded continental US simulations, and 1-year 1-km gridded simulations over central
 458 US agricultural regions (particularly to test individual and combination of physics options related
 459 to crop, irrigation, tile drainage, and groundwater). The tests all showed exactly the same results
 460 between the refactored and base simulations, with similar computational efficiency.

461

462 In addition, in order to provide the community with reference Noah-MP v5.0 model datasets for
463 future comparison and assessment, we have conducted 3 sets of benchmark simulations, including
464 21-year (2000-2020) 12-km continental US simulations driven by the NLDAS-2 atmospheric
465 forcings (Xia et al., 2012), 10-year (2009-2018) point-scale SNOTEL 804-site simulations over
466 the western US driven by observed precipitation and temperature as well as other NLDAS-2
467 atmospheric forcings downscaled to 90-m spatial resolution (He et al., 2021), and 1-year (2000)
468 4-km dynamic crop simulations over the U.S. Corn Belt region driven by the convection-
469 permitting WRF modeling (Zhang et al., 2020). We have archived all the atmospheric forcing
470 datasets, model setup input datasets, and model output datasets for these benchmark simulations.
471 Figure 11 shows an example of the model output. Note that a comprehensive evaluation of the
472 simulation results is outside the scope of this model description paper and will be done in the next
473 step.

474



475

476 **Figure 11.** Demonstration of 20-year (2001-2020) annual mean (a) 2-m temperature, (b) snow
477 cover fraction, (c) snow water equivalent, and (d) top 10-cm soil moisture from the Noah-MP
478 version 5.0 12-km continental US benchmark simulations driven by the NLDAS-2 atmospheric
479 forcings.

480

481 9. Model code and technical documentation for Noah-MP version 5.0

482

483 We archive, manage, and maintain the Noah-MP v5.0 (together with previous code versions) at
484 the NCAR community Noah-MP GitHub repository (<https://github.com/NCAR/noahmp>) for

485 public access. We have also created a comprehensive technical documentation (He et al., 2023)
486 for the Noah-MP v5.0, available at <http://dx.doi.org/10.5065/ew8g-yr95>, which provides detailed
487 descriptions of model physics and formulations.

488

489 10. Conclusions and future plans

490

491 In this study, we modernized the widely-used state-of-the-art Noah-MP LSM by adopting modern
492 Fortran [2003](#) code [standards](#) and data structures, which substantially enhances the model
493 modularity, interoperability, and applicability. The modernized Noah-MP has been released as the
494 model version 5.0, which includes the following key features: (1) enhanced modularization by re-
495 organizing model physics into individual process-level Fortran module files, (2) enhanced data
496 structure with new hierarchical data types and optimized variable declaration and initialization
497 structures, (3) enhanced code structure and calling workflow by leveraging the new data structure
498 and modularization, (4) enhanced (descriptive and self-explanatory) model variable naming
499 standard, and (5) enhanced driver and interface structure to couple with host
500 weather/climate/hydrology models. The base code used for modernization is the Noah-MP version
501 4.5 (released in December 2022), and the modernization effort does not change model physics. In
502 addition, we have created a comprehensive technical documentation (He et al., 2023) of the Noah-
503 MP v5.0, and a set of benchmark simulation datasets.

504

505 The Noah-MP v5.0 has been [recently](#) coupled to the NCAR/HRLDAS system [and the Korean](#)
506 [Integrated Model \(KIM\) system](#). Currently, the work of coupling the Noah-MP v5.0 with the latest
507 NASA/LIS system and the WRF-Hydro/NWM system is on-going. [The future plans for Noah-MP](#)
508 [developments and applications include but not limited to \(1\) coupling with other widely-used](#)
509 [weather/climate models \(e.g., WRF, MPAS, NOAA/UFS\), \(2\) enhancing capability of land data](#)
510 [assimilation with Noah-MP, \(3\) enhancing plant hydraulics and soil hydraulics/hydrology schemes,](#)
511 [\(4\) improving accuracy of applications in subseasonal-to-seasonal \(S2S\) forecasts, food-water](#)
512 [security, and extreme weather/climate \(e.g., fire, drought, flood, and heatwave\), \(5\) including](#)
513 [automated model parameter calibration/optimization algorithms, \(6\) enhancing modeling](#)
514 [capabilities for rapid landscape transformation \(e.g., deforestation/reforestation\) as well as](#)
515 [vegetation recovery and replacement after environmental disturbance, \(7\) including human](#)
516 [management modeling \(e.g., groundwater pumping\), \(8\) including interactions with air pollution](#)
517 [\(e.g., pollutants' deposition and ozone damage to vegetation\), \(9\) enhancing representation of](#)
518 [subgrid heterogeneity, \(10\) improving high-resolution input datasets \(e.g., soil properties and](#)
519 [groundwater-related inputs\), and \(11\) creating a set of packages for code benchmarking and testing,](#)
520 [model diagnostic, and better debugging capability.](#) Overall, the modernized open-source
521 community Noah-MP model [allows](#) a more efficient and convenient process for future model
522 developments and applications.

523

524

Deleted: and standards

Deleted: and interoperability

Deleted: In the future, we also plan to couple the Noah-MP v5.0 to other weather and climate models, including WRF, MPAS, and NOAA/UFS.

Deleted: will

Formatted: Font: (Asian) Times New Roman

531 **Code and data availability**

532 1. The Noah-MP model code (<https://doi.org/10.5281/zenodo.7901855>) is available at
533 <https://github.com/NCAR/noahmp>

534 2. The coupled HRLDAS/Noah-MP model code (<https://doi.org/10.5281/zenodo.7901867>) is
535 available at <https://github.com/NCAR/hrlDas>

536 3. The Noah-MP technical documentation is available at <http://dx.doi.org/10.5065/ew8g-yr95>

537 4. The benchmark datasets are stored in the NCAR high-performance supercomputer (HPC)
538 campaign storage file system (data path: /glade/campaign/ral/hap/cenlinhe/NoahMP_benchmark/,
539 see details about the storage system at https://arc.ucar.edu/knowledge_base/70549621) and can be
540 provided by the corresponding author upon request, due to the extremely large data size (8.8 TB).

541

542

543 **Author contribution**

544 CH, PV, and MB led the code refactoring effort with the help from all the other coauthors (FC,
545 DG, RC, GN, ZY, DN, ME, TS, RR). CH and PV led the technical documentation writing effort
546 with the help from all the other coauthors (MB, FC, DG, RC, GN, ZY, DN, ME, TS, RR). CH
547 conducted the benchmark model simulations. CH drafted the manuscript with improvements from
548 all the other coauthors (PV, FC, MB, DG, RC, GN, ZY, DN, ME, TS, RR).

549

550

551 **Competing interests**

552 The authors declare that they have no conflict of interest.

553

554

555 **Acknowledgements**

556 We thank Zhe Zhang (NCAR) and Ronnie Abolafia-Rosenzweig (NCAR) for helping with model
557 code testing and for helpful discussions. We also acknowledge the strong support from the entire
558 Noah-MP community. This study was supported by the US Geological Survey (USGS) Water
559 Mission Area's Integrated Water Prediction Program, NOAA's Climate Program Office's
560 Modeling, Analysis, Predictions, and Projections Program (MAPP), and the NCAR Water System
561 Program. National Center for Atmospheric Research (NCAR) is a major facility sponsored by the
562 National Science Foundation (NSF) under Cooperative Agreement #1852977. Any opinions,
563 findings, conclusions, or recommendations expressed in this publication are those of the authors
564 and do not necessarily reflect the views of the National Science Foundation.

565

566

567 **References**

568 Abolafia-Rosenzweig, R., He, C., Burns, S.P., Chen, F., 2021. Implementation and Evaluation of
569 a Unified Turbulence Parameterization Throughout the Canopy and Roughness Sublayer in

570 Noah-MP Snow Simulations. *J Adv Model Earth Syst* 13.
571 <https://doi.org/10.1029/2021MS002665>

572 Abolafia-Rosenzweig, R., He, C., Chen, F., 2022a. Winter and spring climate explains a large
573 portion of interannual variability and trend in western U.S. summer fire burned area. *Environ.*
574 *Res. Lett.* 17, 054030. <https://doi.org/10.1088/1748-9326/ac6886>

575 Abolafia-Rosenzweig, R., He, C., McKenzie Skiles, S., Chen, F., Gochis, D., 2022b. Evaluation
576 and Optimization of Snow Albedo Scheme in Noah-MP Land Surface Model Using In Situ
577 Spectral Observations in the Colorado Rockies. *J Adv Model Earth Syst* 14.
578 <https://doi.org/10.1029/2022MS003141>

579 Abolafia-Rosenzweig, R., He, C., Chen, F. et al. 2023a. High Resolution Forecasting of Summer
580 Drought in the Western United States. *Water Resources Research*, in review

581 Abolafia-Rosenzweig, R., He, C., Chen, F. et al. 2023b. Evaluating Noah-MP simulated post-fire
582 runoff and snowpack in Pacific-Northwest: challenges and future improvements, *Water*
583 *Resources Research*, in review

584 Anderson, E. A. (1976), A point energy and mass balance model of a snow cover, NOAA Tech.
585 Rep. NWS 19, 150 pp., Off. of Hydrol., Natl. Weather Serv., Silver Spring, Md.

586 Arsenault, K. R., Shukla, S., Hazra, A., Getirana, A., McNally, A., Kumar, S. V., ... & Verdin, J.
587 P. (2020). Better Advance Warnings of Drought. *Bulletin of the American Meteorological*
588 *Society*, 101(10), 899-903.

589 Ball, J. T., I. E. Woodrow, and J. A. Berry (1987), A model predicting sto- matal conductance and
590 its contribution to the control of photosynthesis under different environmental conditions, in
591 *Process in Photosynthesis Research*, vol. 1, edited by J. Biggins, pp. 221–234, Martinus Nijhoff,
592 Dordrecht, Netherlands.

593 Barlage, M., Tewari, M., Chen, F., Miguez-Macho, G., Yang, Z. L., & Niu, G. Y. (2015). The
594 effect of groundwater interaction in North American regional climate simulations with
595 WRF/Noah-MP. *Climatic Change*, 129, 485-498.

596 Barlage, M., Chen, F., Rasmussen, R., Zhang, Z., & Miguez-Macho, G. (2021). The importance
597 of scale-dependent groundwater processes in land-atmosphere interactions over the central
598 United States. *Geophysical Research Letters*, 48(5), e2020GL092171.

599 Blyth, E. M., Arora, V. K., Clark, D. B., Dadson, S. J., De Kauwe, M. G., Lawrence, D. M., ... &
600 Yuan, H. (2021). Advances in land surface modelling. *Current Climate Change Reports*, 7(2),
601 45-71.

602 Bonan, G. B. (1996), A land surface model (LSM version 1.0) for ecolog- ical, hydrological, and
603 atmospheric studies: Technical description and user's guide, NCAR Tech. Note NCAR/TN-
604 417+STR, 150 pp., Natl. Cent. for Atmos. Res., Boulder, Colo.

605 Bonan, G. B., & Doney, S. C. (2018). Climate, ecosystems, and planetary futures: The challenge
606 to predict life in Earth system models. *Science*, 359(6375), eaam8328.
607 <https://doi.org/10.1126/science.aam8328>

608 Brunsell, N. A., de Oliveira, G., Barlage, M., Shimabukuro, Y., Moraes, E., & Aragao, L. (2021).
609 Examination of seasonal water and carbon dynamics in eastern Amazonia: a comparison of
610 Noah-MP and MODIS. *Theoretical and Applied Climatology*, 143, 571-586.

611 Brutsaert, W. A. (1982), *Evaporation Into the Atmosphere*, 299 pp., D. Reidel, Dordrecht,
612 Netherlands.

613 Cai, X., Yang, Z. L., David, C. H., Niu, G. Y., & Rodell, M. (2014). Hydrological evaluation of
614 the Noah-MP land surface model for the Mississippi River Basin. *Journal of Geophysical*
615 *Research: Atmospheres*, 119(1), 23-38.

616 Cai, X., Yang, Z. L., Fisher, J. B., Zhang, X., Barlage, M., & Chen, F. (2016). Integration of
617 nitrogen dynamics into the Noah-MP land surface model v1. 1 for climate and environmental
618 predictions. *Geoscientific Model Development*, 9(1), 1-15.

619 Chang, M., Cao, J., Zhang, Q., Chen, W., Wu, G., Wu, L., ... & Wang, X. (2022). Improvement of
620 stomatal resistance and photosynthesis mechanism of Noah-MP-WDDM (v1. 42) in simulation
621 of NO₂ dry deposition velocity in forests. *Geoscientific Model Development*, 15(2), 787-801.

622 Chen, F., & Dudhia, J. (2001). Coupling an advanced land surface–hydrology model with the Penn
623 State–NCAR MM5 Modeling System. Part I: Model implementation and sensitivity. *Monthly*
624 *Weather Review*, 129, 17. [https://doi.org/10.1175/1520-0493\(2001\)129<0569:caalsh>2.0.co;2](https://doi.org/10.1175/1520-0493(2001)129<0569:caalsh>2.0.co;2)

625 Chen, F., Janjić, Z., & Mitchell, K. (1997). Impact of atmospheric surface-layer parameterizations
626 in the new land-surface scheme of the NCEP Mesoscale Eta Model. *Boundary-Layer*
627 *Meteorology*, 85, 391–421. <https://doi.org/10.1023/A:1000531001463>

628 Chen, F., Mitchell, K., Schaake, J., Xue, Y., Pan, H.-L., Koren, V., et al. (1996). Modeling of land
629 surface evaporation by four schemes and comparison with FIFE observations. *Journal of*
630 *Geophysical Research: Atmospheres*, 101, 7251–7268. <https://doi.org/10.1029/95JD02165>

631 Chen, F., & Zhang, Y. (2009). On the coupling strength between the land surface and the
632 atmosphere: From viewpoint of surface exchange coefficients. *Geophysical Research*
633 *Letters*, 36(10).

634 Chen, L., Li, Y., Chen, F., Barr, A., Barlage, M., & Wan, B. (2016). The incorporation of an
635 organic soil layer in the Noah-MP land surface model and its evaluation over a boreal aspen
636 forest. *Atmospheric Chemistry and Physics*, 16(13), 8375-8387.

637 Dickinson, R. E. (1983), Land surface processes and climate-surface albedo and energy balance,
638 in *Theory of Climate*, *Adv. Geophys.*, vol. 25, edited by B. Saltzman, pp. 305–353, Academic,
639 San Diego, Calif.

640 Dickinson, R. E., A. Henderson-Sellers, and P. J. Kennedy (1993), Bio- sphere-Atmosphere
641 Transfer Scheme (BATS) version 1e as coupled to the NCAR Community Climate Model,
642 NCAR Tech. Note NCAR/TN- 387+STR, 80 pp., Natl. Cent. for Atmos. Res., Boulder, Colo.

643 Dickinson, R. E., M. Shaikh, R. Bryant, and L. Graumlich (1998), Interac- tive canopies for a
644 climate model, *J. Clim.*, 11, 2823–2836, doi:10.1175/ 1520-
645 0442(1998)011<2823:ICFACM>2.0.CO;2.

646 Ek, M. B., Mitchell, K. E., Lin, Y., Rogers, E., Grunmann, P., Koren, V., et al. (2003).
647 Implementation of Noah land surface model advances in the National Centers for

648 Environmental Prediction operational mesoscale Eta model. *Journal of Geophysical Research:*
649 *Atmospheres*, 108, 2002JD003296. <https://doi.org/10.1029/2002JD003296>

650 Fan, Y., Miguez-Macho, G., Weaver, C. P., Walko, R., & Robock, A. (2007). Incorporating water
651 table dynamics in climate modeling: 1. Water table observations and equilibrium water table
652 simulations. *Journal of Geophysical Research: Atmospheres*, 112(D10).

653 Gao, Y., Xiao, L., Chen, D., Chen, F., Xu, J., & Xu, Y. (2017). Quantification of the relative role
654 of land-surface processes and large-scale forcing in dynamic downscaling over the Tibetan
655 Plateau. *Climate Dynamics*, 48, 1705-1721.

656 Hazra, A., McNally, A., Slinski, K., Arsenault, K. R., Shukla, S., Getirana, A., ... & Koster, R. D.
657 (2023). NASA's NMME-based S2S hydrologic forecast system for food insecurity early
658 warning in southern Africa. *Journal of Hydrology*, 617, 129005.

659 He, C., F. Chen, M. Barlage, C. Liu, A. Newman, W. Tang, K. Ikeda, and R. Rasmussen (2019):
660 Can convection-permitting modeling provide decent precipitation for offline high-resolution
661 snowpack simulations over mountains, *J. Geophys. Res.-Atmos*,
662 124, <https://doi.org/10.1029/2019JD030823>

663 He, C., F. Chen, R. Abolafia-Rosenzweig, K. Ikeda, C. Liu, and R. Rasmussen (2021): What
664 causes the unobserved early-spring snowpack ablation in convection-permitting WRF modeling
665 over Utah mountains?, *J. Geophys. Res.-Atmos*, 126(22),
666 e2021JD035284, <https://doi.org/10.1029/2021JD035284>

667 He, C., P. Valayamkunnath, M. Barlage, F. Chen, D. Gochis, R. Cabell, T. Schneider, R.
668 Rasmussen, G.-Y. Niu, Z.-L. Yang, D. Niyogi, and M. Ek (2023): The Community Noah-MP
669 Land Surface Modeling System Technical Description Version 5.0. (*No. NCAR/TN-575+STR*),
670 <http://dx.doi.org/10.5065/ew8g-yr95>

671 Ingwersen, J., Högy, P., Wizemann, H. D., Warrach-Sagi, K., & Streck, T. (2018). Coupling the
672 land surface model Noah-MP with the generic crop growth model Gecros: Model description,
673 calibration and validation. *Agricultural and forest meteorology*, 262, 322-339.

674 Jarvis, P. G. (1976). The interpretation of the variations in leaf water poten- tial and stomatal
675 conductance found in canopies in the field, *Philos. Trans. R. Soc. B*, 273, 593–610,
676 doi:10.1098/rstb.1976.0035.

677 Jayawardena, A. W. and Zhou, M. C.: A modified spatial soil moisture storage capacity
678 distribution curve for the Xinanjiang model, *Journal of Hydrology*, 227, 93–113,
679 [https://doi.org/10.1016/S0022-1694\(99\)00173-0](https://doi.org/10.1016/S0022-1694(99)00173-0), 2000.

680 Jiang, Y., Chen, F., Gao, Y., He, C., Barlage, M., & Huang, W. (2020). Assessment of uncertainty
681 sources in snow cover simulation in the Tibetan Plateau. *Journal of Geophysical Research:*
682 *Atmospheres*, 125(18), e2020JD032674.

683 Jiang, Y., Gao, Y., He, C., Liu, B., Pan, Y., & Li, X. (2021). Spatiotemporal distribution and
684 variation of wind erosion over the Tibetan Plateau based on a coupled land-surface wind-
685 erosion model. *Aeolian Research*, 50, 100699.

686 Jordan, R. (1991), A one-dimensional temperature model for a snow cover, *Spec. Rep. 91–16*,
687 Cold Reg. Res. and Eng. Lab., U.S. Army Corps of Eng., Hanover, N. H.

688 Ju, C., Li, H., Li, M., Liu, Z., Ma, Y., Mamtimin, A., ... & Song, Y. (2022). Comparison of the
689 Forecast Performance of WRF Using Noah and Noah-MP Land Surface Schemes in Central
690 Asia Arid Region. *Atmosphere*, 13(6), 927.

691 Koren, V., J. C. Schaake, K. E. Mitchell, Q.-Y. Duan, F. Chen, and J. M. Baker (1999), A
692 parameterization of snowpack and frozen ground intended for NCEP weather and climate
693 models, *J. Geophys. Res.*, 104, 19,569–19,585, doi:10.1029/1999JD900232.

694 Kumar, S. V., Mocko, D. M., Wang, S., Peters-Lidard, C. D., & Borak, J. (2019). Assimilation of
695 remotely sensed leaf area index into the Noah-MP land surface model: Impacts on water and
696 carbon fluxes and states over the continental United States. *Journal of*
697 *Hydrometeorology*, 20(7), 1359-1377.

698 Kumar, S. V., Holmes, T., Andela, N., Dharssi, I., Hain, C., Peters-Lidard, C., ... & Getirana, A.
699 (2021). The 2019–2020 Australian drought and bushfires altered the partitioning of
700 hydrological fluxes. *Geophysical Research Letters*, 48(1), e2020GL091411.

701 Li, X., Wu, T., Zhu, X., Jiang, Y., Hu, G., Hao, J., ... & Ying, X. (2020). Improving the Noah-MP
702 model for simulating hydrothermal regime of the active layer in the permafrost regions of the
703 Qinghai-Tibet Plateau. *Journal of Geophysical Research: Atmospheres*, 125(16),
704 e2020JD032588.

705 Li, J., Chen, F., Lu, X., Gong, W., Zhang, G., & Gan, Y. (2020). Quantifying contributions of
706 uncertainties in physical parameterization schemes and model parameters to overall errors in
707 Noah-MP dynamic vegetation modeling. *Journal of Advances in Modeling Earth Systems*, 12.
708 <https://doi.org/10.1029/2019MS001914>

709 Li, L., Yang, Z. L., Matheny, A. M., Zheng, H., Swenson, S. C., Lawrence, D. M., ... & Leung, L.
710 R. (2021). Representation of plant hydraulics in the Noah-MP land surface model: Model
711 development and multiscale evaluation. *Journal of Advances in Modeling Earth Systems*, 13(4),
712 e2020MS002214.

713 Li, M., Wu, P., Ma, Z., Lv, M., Yang, Q., & Duan, Y. (2022). The decline in the groundwater table
714 depth over the past four decades in China simulated by the Noah-MP land model. *Journal of*
715 *Hydrology*, 607, 127551.

716 Liang, J., Yang, Z., & Lin, P. (2019). Systematic hydrological evaluation of the Noah-MP land
717 surface model over China. *Advances in Atmospheric Sciences*, 36, 1171-1187.

718 Liang, X., Lettenmaier, D. P., Wood, E. F., & Burges, S. J. (1994). A simple hydrologically based
719 model of land surface water and energy fluxes for general circulation models. *Journal of*
720 *Geophysical Research: Atmospheres*, 99(D7), 14415-14428.

721 Liang, X., & Xie, Z. (2003). Important factors in land-atmosphere interactions: surface runoff
722 generations and interactions between surface and groundwater. *Global and Planetary Change*,
723 38(1-2), 101-114.

724 Liu, C., Ikeda, K., Rasmussen, R., Barlage, M., Newman, A. J., Prein, A. F., ... & Yates, D. (2017).
725 Continental-scale convection-permitting modeling of the current and future climate of North
726 America. *Climate Dynamics*, 49, 71-95.

Formatted: Font: (Default) Times New Roman, 12 pt

Formatted: Font: (Default) Times New Roman, 12 pt

727 Liu, X., Chen, F., Barlage, M., Zhou, G., & Niyogi, D. (2016). Noah-MP-Crop: Introducing
728 dynamic crop growth in the Noah-MP land surface model. *Journal of Geophysical Research:*
729 *Atmospheres*, 121(23), 13-953.

730 McDaniel, R., Liu, Y., Valayamkunnath, P., Barlage, M., Gochis, D., Cosgrove, B. A., & Flowers,
731 T. (2020, December). Moisture condition impact and seasonality of National Water Model
732 performance under different runoff-infiltration partitioning schemes. In *AGU Fall Meeting*
733 *Abstracts* (Vol. 2020, pp. H111-0028).

734 Miguez-Macho, G., Fan, Y., Weaver, C. P., Walko, R., & Robock, A. (2007). Incorporating water
735 table dynamics in climate modeling: 2. Formulation, validation, and soil moisture
736 simulation. *Journal of Geophysical Research: Atmospheres*, 112(D13).

737 Nie, W., Kumar, S. V., Arsenault, K. R., Peters-Lidard, C. D., Mladenova, I. E., Bergaoui, K., ...
738 & Navari, M. (2022). Towards effective drought monitoring in the Middle East and North
739 Africa (MENA) region: implications from assimilating leaf area index and soil moisture into
740 the Noah-MP land surface model for Morocco. *Hydrology and Earth System Sciences*, 26(9),
741 2365-2386.

742 Niu, G.-Y., and Z.-L. Yang (2004), The effects of canopy processes on snow surface energy and
743 mass balances, *J. Geophys. Res.*, 109, D23111, doi:10.1029/2004JD004884.

744 Niu, G.-Y., Z.-L. Yang, R. E. Dickinson, and L. E. Gulden (2005), A simple TOPMODEL-based
745 runoff parameterization (SIMTOP) for use in global climate models, *J. Geophys. Res.*, 110,
746 D21106, doi:10.1029/2005JD006111.

747 Niu, G.-Y., and Z.-L. Yang (2006), Effects of frozen soil on snowmelt runoff and soil water
748 storage at a continental scale, *J. Hydrometeorol.*, 7, 937–952, doi:10.1175/JHM538.1.

749 Niu, G.-Y., Z.-L. Yang, R. E. Dickinson, L. E. Gulden, and H. Su (2007), Development of a simple
750 groundwater model for use in climate models and evaluation with Gravity Recovery and
751 Climate Experiment data, *J. Geophys. Res.*, 112, D07103, doi:10.1029/2006JD007522.

752 Niu, G.-Y., Yang, Z.-L., Mitchell, K. E., Chen, F., Ek, M. B., Barlage, M., et al. (2011). The
753 community Noah land surface model with multiparameterization options (Noah-MP): 1.
754 Model description and evaluation with local-scale measurements. *Journal of Geophysical*
755 *Research*, 116, D12109. <https://doi.org/10.1029/2010JD015139>

756 Niu, G. Y., Fang, Y. H., Chang, L. L., Jin, J., Yuan, H., & Zeng, X. (2020). Enhancing the Noah-
757 MP ecosystem response to droughts with an explicit representation of plant water storage
758 supplied by dynamic root water uptake. *Journal of Advances in Modeling Earth*
759 *Systems*, 12(11), e2020MS002062.

760 Oleson, K. W., et al. (2004), Technical description of the Community Land Model (CLM), NCAR
761 Tech. Note NCAR/TN-461+STR, 174 pp., Natl. Cent. for Atmos. Res., Boulder, Colo.
762 (Available at www.cgd.ucar.edu/tss/clm/distribution/clm3.0/index.html.)

763 Patel, P., Jamshidi, S., Nadimpalli, R., Aliaga, D. G., Mills, G., Chen, F., ... & Niyogi, D. (2022).
764 Modeling Large-Scale Heatwave by Incorporating Enhanced Urban Representation. *Journal of*
765 *Geophysical Research: Atmospheres*, 127(2), e2021JD035316.

766 Sakaguchi, K., & Zeng, X. (2009). Effects of soil wetness, plant litter, and under-canopy
767 atmospheric stability on ground evaporation in the Community Land Model (CLM3. 5). *Journal*
768 *of Geophysical Research: Atmospheres*, 114(D1).

769 Salamanca, F., Zhang, Y., Barlage, M., Chen, F., Mahalov, A., & Miao, S. (2018). Evaluation of
770 the WRF-urban modeling system coupled to Noah and Noah-MP land surface models over a
771 semiarid urban environment. *Journal of Geophysical Research: Atmospheres*, 123(5), 2387-
772 2408.

773 Saxton, K. E., & Rawls, W. J. (2006). Soil water characteristic estimates by texture and organic
774 matter for hydrologic solutions. *Soil science society of America Journal*, 70(5), 1569-1578.

775 Sellers, P. J. (1985). Canopy reflectance, photosynthesis and transpiration, *Int. J. Remote Sens.*, 6,
776 1335–1372, doi:10.1080/01431168508948283.

777 Sellers, P. J., M. D. Heiser, and F. G. Hall (1992), Relations between surface conductance and
778 spectral vegetation indices at intermediate (100 m² to 15 km²) length scales, *J. Geophys. Res.*,
779 97, 19,033–19,059, doi:10.1029/92JD01096.

780 Schaake, J. C., V. I. Koren, Q.-Y. Duan, K. E. Mitchell, and F. Chen (1996), Simple water balance
781 model for estimating runoff at different spatial and temporal scales, *J. Geophys. Res.*, 101,
782 7461–7475, doi:10.1029/95JD02892.

783 [Shu, Z., Zhang, B., Tian, L., & Zhao, X. \(2022\). Improving Dynamic Vegetation Modeling in
784 Noah - MP by Parameter Optimization and Data Assimilation Over China's Loess
785 Plateau. *Journal of Geophysical Research: Atmospheres*, 127\(19\), e2022JD036703.](#)

786 Suzuki, K., & Zupanski, M. (2018). Uncertainty in solid precipitation and snow depth prediction
787 for Siberia using the Noah and Noah-MP land surface models. *Frontiers of Earth Science*, 12,
788 672-682.

789 Valayamkunnath, P., Chen, F., Barlage, M. J., Gochis, D. J., Franz, K. J., & Cosgrove, B. A. (2021,
790 January). Impact of Agriculture Management Practices on the National Water Model Simulated
791 Streamflow. In 101st American Meteorological Society Annual Meeting. AMS.

792 Valayamkunnath, P., Gochis, D. J., Chen, F., Barlage, M., & Franz, K. J. (2022). Modeling the
793 hydrologic influence of subsurface tile drainage using the National Water Model. *Water*
794 *Resources Research*, 58(4), e2021WR031242.

795 Verseghy, D. L. (1991), CLASS-A Canadian land surface scheme for GCMS: I. Soil model, *Int. J.*
796 *Climatol.*, 11, 111–133, doi:10.1002/joc.3370110202.

797 Wang, P., Niu, G. Y., Fang, Y. H., Wu, R. J., Yu, J. J., Yuan, G. F., ... & Scott, R. L. (2018).
798 Implementing dynamic root optimization in Noah-MP for simulating phreatophytic root water
799 uptake. *Water Resources Research*, 54(3), 1560-1575.

800 Wang, W., Yang, K., Zhao, L., Zheng, Z., Lu, H., Mamtimin, A., ... & Moore, J. C. (2020).
801 Characterizing surface albedo of shallow fresh snow and its importance for snow ablation on
802 the interior of the Tibetan Plateau. *Journal of Hydrometeorology*, 21(4), 815-827.

803 Wang, W., He, C., Moore, J., Wang, G., & Niu, G. Y. (2022). Physics-Based Narrowband Optical
804 Parameters for Snow Albedo Simulation in Climate Models. *Journal of Advances in Modeling*
805 *Earth Systems*, 14(1), e2020MS002431.

Formatted: Font: (Default) Times New Roman, 12 pt

806 Wang, Y. H., Broxton, P., Fang, Y., Behrangi, A., Barlage, M., Zeng, X., & Niu, G. Y. (2019). A
807 wet-bulb temperature-based rain-snow partitioning scheme improves snowpack prediction over
808 the drier western United States. *Geophysical Research Letters*, 46(23), 13825-13835.

809 Warrach-Sagi, K., J. Ingwersen, T. Schwitalla, C. Troost, J. Aurbacher, L. Jach, T. Berger, T.
810 Streck, and V. Wulfmeyer, 2022: Noah-MP with the generic crop growth model Gecros in the
811 WRF model: Effects of dynamic crop growth on land-atmosphere interaction. *J Geophys Res-*
812 *Atmos*, 127(14), e2022JD036518.DOI:10.1029/2022JD036518

813 Wrzesien, M. L., Pavelsky, T. M., Kapnick, S. B., Durand, M. T., & Painter, T. H. (2015).
814 Evaluation of snow cover fraction for regional climate simulations in the Sierra Nevada.
815 *International Journal of Climatology*, 35(9), 2472-2484.

816 Wu, W. Y., Yang, Z. L., & Barlage, M. (2021). The Impact of Noah-MP Physical
817 Parameterizations on Modeling Water Availability during Droughts in the Texas–Gulf
818 Region. *Journal of Hydrometeorology*, 22(5), 1221-1233.

819 Xia, Y., K. Mitchell, M. Ek, J. Sheffield, B. Cosgrove, E. Wood, L. Luo, C. Alonge, H. Wei, J.
820 Meng, B. Livneh, D. Lettenmaier, V. Koren, Q. Duan, K. Mo, Y. Fan, and D. Mocko (2012).
821 Continental-scale water and energy flux analysis and validation for the North American Land
822 Data Assimilation System project phase 2 (NLDAS-2): 1. Intercomparison and application of
823 model products. *J. Geophys. Res.*, 117, D03109, doi:10.1029/2011JD016048

824 Xu, T., Chen, F., He, X., Barlage, M., Zhang, Z., Liu, S., & He, X. (2021). Improve the
825 performance of the noah-MP-crop model by jointly assimilating soil moisture and vegetation
826 phenology data. *Journal of Advances in Modeling Earth Systems*, 13(7), e2020MS002394.

827 Xu, X., Chen, F., Shen, S., Miao, S., Barlage, M., Guo, W., & Mahalov, A. (2018). Using WRF-
828 urban to assess summertime air conditioning electric loads and their impacts on urban weather
829 in Beijing. *Journal of Geophysical Research: Atmospheres*, 123(5), 2475-2490.

830 Xue, Y., P. J. Sellers, J. L. Kinter, and J. Shukla (1991), A simplified bio- sphere model for global
831 climate studies, *J. Clim.*, 4, 345–364, doi:10.1175/1520-
832 0442(1991)004<0345:ASBMFG>2.0.CO;2.

833 Yang, Z.-L., and R. E. Dickinson (1996), Description of the Biosphere- Atmosphere Transfer
834 Scheme (BATS) for the soil moisture workshop and evaluation of its performance, *Global*
835 *Planet. Change*, 13, 117–134, doi:10.1016/0921-8181(95)00041-0.

836 Yang, Z. L., Niu, G. Y., Mitchell, K. E., Chen, F., Ek, M. B., Barlage, M., ... & Xia, Y. (2011).
837 The community Noah land surface model with multiparameterization options (Noah-MP): 2.
838 Evaluation over global river basins. *Journal of Geophysical Research: Atmospheres*, 116(D12).

839 Yen, Y. C. (1965). Effective thermal conductivity and water vapor diffusivity of naturally
840 compacted snow. *Journal of Geophysical Research*, 70(8), 1821-1825.

841 Yen, Y. C. (1981). Review of thermal properties of snow, ice, and sea ice (Vol. 81, No. 10). US
842 Army, Corps of Engineers, Cold Regions Research and Engineering Laboratory.

843 Zhang, G., Chen, F., & Gan, Y. (2016). Assessing uncertainties in the Noah-MP ensemble
844 simulations of a cropland site during the Tibet Joint International Cooperation program field

845 campaign. *Journal of Geophysical Research: Atmospheres*, 121, 9576–9596. <https://doi.org/10.1002/2016JD024928>
846

847 Zhang, X. Y., Jin, J., Zeng, X., Hawkins, C. P., Neto, A. A., & Niu, G. Y. (2022a). The
848 compensatory CO₂ fertilization and stomatal closure effects on runoff projection from 2016–
849 2099 in the western United States. *Water Resources Research*, 58(1), e2021WR030046.

850 Zhang, X., Xie, Z., Ma, Z., Barron-Gafford, G. A., Scott, R. L., & Niu, G. Y. (202b). A Microbial-
851 Explicit Soil Organic Carbon Decomposition Model (MESDM): Development and Testing at a
852 Semiarid Grassland Site. *Journal of Advances in Modeling Earth Systems*, 14(1),
853 e2021MS002485.

854 Zhang, Z., Barlage, M., Chen, F., Li, Y., Helgason, W., Xu, X., ... & Li, Z. (2020). Joint modeling
855 of crop and irrigation in the central United States using the Noah-MP land surface
856 model. *Journal of Advances in Modeling Earth Systems*, 12(7), e2020MS002159.

857 Zhang, Z., Chen, F., Barlage, M., Bortolotti, L. E., Famiglietti, J., Li, Z., ... & Li, Y. (2022).
858 Cooling Effects Revealed by Modeling of Wetlands and Land-Atmosphere Interactions. *Water*
859 *Resources Research*, 58(3), e2021WR030573.

860 Zhang, Z., Li, Y., Chen, F., Harder, P., Helgason, W., Famiglietti, J., Valayamkunnath, P., He, C.,
861 and Li, Z.: Developing Spring Wheat in the Noah-MP LSM (v4.4) for Growing Season
862 Dynamics and Responses to Temperature Stress, *Geosci. Model Dev. Discuss.* [preprint],
863 <https://doi.org/10.5194/gmd-2022-311>, in review, 2023.

864 Zhuo, L., Dai, Q., Han, D., Chen, N., & Zhao, B. (2019). Assessment of simulated soil moisture
865 from WRF Noah, Noah-MP, and CLM land surface schemes for landslide hazard
866 application. *Hydrology and Earth System Sciences*, 23(10), 4199-4218.

867 Zonato, A., Martilli, A., Gutierrez, E., Chen, F., He, C., Barlage, M., ... & Giovannini, L. (2021).
868 Exploring the effects of rooftop mitigation strategies on urban temperatures and energy
869 consumption. *Journal of Geophysical Research: Atmospheres*, 126(21), e2021JD035002.
870